Pakistan J. Zool., pp 1-10, 2025. **DOI**: https://dx.doi.org/10.17582/journal.pjz/20240726135052

Exploring the Effect of Zinc Oxide Nanoparticles Extracted from *Tribulus terrestris* on Alloxan-Induced Diabetic Mice

Hafiza Sadaf Zahra[1], Riffat Iqbal[2]* and Muhammad Khan[1]*

[1]*Institute of Zoology, University of the Punjab, Quaid-e-Azam Campus Lahore-54590, Pakistan*
[2]*Department of Zoology, Government College University, Lahore-54000, Pakistan*

ABSTRACT

Diabetes, characterized by high levels of glucose in the blood, imposes significant health and economic burdens globally. The current study aimed to develop a potent antidiabetic drug with fewer adverse effects. Therefore, zinc oxide nanoparticles (ZnONPs) were prepared using green methods from *Tribulus terrestris* fruit extract and the characterization was done using UV, FTIR, SEM, XRD, and EDX. *Tribulus terrestris*-synthesized zinc oxide nanoparticles (TT-ZnONPs) were used to measure the antidiabetic efficacy in alloxan-induced diabetic mice divided into six groups. Group A (negative control), Group B (untreated diabetic control) Group C (10 mg/kg glibenclamide), and Groups D, E, and F (10, 20 and 30 mg/kg TT-ZnONPs) for diabetic mice treatments. Results showed dose-dependent blood glucose level reduction with 10, 20 and 30 mg/kg TT-ZnONPs. Additionally, significant dose-dependent reductions in lipid profile markers along with a remarkable increase in high density lipoprotein-cholesterol were observed. Liver function markers exhibited a notable decrease while total protein demonstrated a significant increase. Furthermore, the renal function markers (urea, uric acid, creatinine, and albumin) were significantly decreased. The levels of various haematological parameters in treatment groups were comparable to untreated control. Histopathological analysis showed remarkable dose-dependent improvements in the pancreas, liver, and kidney structure compared to the untreated diabetic group. It was worth mentioning that the antidiabetic effect of TT-ZnONPs was significantly higher compared to glibenclamide. Therefore, TT-ZnONPs have the potential for effective pharmaceutical formulation for the management of DM.

Article Information
Received 26 July 2024
Revised 05 April 2025
Accepted 18 April 2025
Available online 11 June 2025
(early access)

Authors' Contribution
HSZ and MK designed the study. HSZ performed the experiment and wrote the manuscript. RI and MK interpreted and analyzed the data. All authors approved the final version of the manuscript.

Key words
***Tribulus terrestris*, ZnO nanoparticles, Biochemical parameters, Hematology, Diabetes, Green nanotechnology**

INTRODUCTION

Nanotechnology plays an important role in the detection and management of diabetes (Rajam, 2024; Virk, 2018). A major advancement in diabetes treatment is the creation of innovative nano-sensors, which make it simple, precise, and sensitive to test blood sugar. The intravenous insulin infusion through nanotechnology, circumventing gastric acidity, thereby serving as a substitute for daily subcutaneous injections (DiSanto *et al*., 2015). In recent years, innovative delivery methods to improve diabetes treatment have achieved ground-breaking in nanotechnology. It is utilized to address significant shortcomings of contemporary medications, such as their low bioavailability and rapid onset of undesired side effects upon entering the bloodstream (Simos *et al*., 2021).

Due to their remarkable electrical, optical, magnetic, and catalytic capabilities, metal and metal oxide nanoparticles (MNPs and MONPs) are a major focus of research. Copper, gold, silver, zinc, iron, titanium, and platinum are a small part of the diverse types of MNPs and MONPs (Khan *et al*., 2021; Azeem and Abdel-Megid, 2023). These have received much attention because of the relative improvements in diagnosing and managing life-threatening diseases (Chandrakala *et al*., 2022; Shafey, 2020).

In this study, *Tribulus terrestris* fruit extract (TTFE), which exhibited antidiabetic properties, was incorporated into the process of developing ZnONPs that are a combination of the *T. terrestris* antidiabetic characteristics and special peculiarities of nanoparticles to potentially offer a solution against diabetes. TTFE is rich in bioactive components that possess antioxidant and antihyperglycemic activities (Stefanescu *et al*., 2021; Bouzekri *et al*., 2024). When it is incorporated in the preparation of ZnONPs, the collective approach of this

* Corresponding author: mkhan.zool@pu.edu.pk, riffatiqbal@gcu.edu.pk
0030-9923/2025/0001-0001 $ 9.00/0

extract could help boost the fight against glucose levels, raise insulin responsiveness, prevent oxidation, and protect the pancreatic beta cells (Amin *et al*., 2006). Because of its capacity to control aspects of diabetes care and promote blood glucose homeostasis, these attributes together make it highly valuable (Kamtekar and Keer, 2014; Bonakdaran *et al*., 2008).

This experiment aimed to determine the mechanism that would open the door to a natural method of managing type 2 diabetes and the effectiveness of TT-ZnONPs in the regulation of BGLs.

MATERIALS AND METHODS

Synthesis and characterization of ZnONPs from T. terrrestris

The fruit of the *T. terrestris* plant (voucher specimen labeled as G.C. Herb., Bot.-3297) was rinsed thoroughly with water, sun-dried for approximately 2 weeks, and ground into a fine powder. Five g of this powder was suspended in 100 ml of pure water, boiled, cooled at room temperature (Gopinath *et al*., 2016), and then filtered using Whatman (No.1) filter paper for preparation of zinc oxide nanoparticle (ZnONPs) from *T. terrestris* according to Hameed *et al*. (2021). Various techniques (UV-Vis, FTIR, XRD, SEM, and EDX) were utilized to examine the attributes of the *T. terrestris* synthesized zinc oxide nanoparticles (TT-ZnONPs).

In vivo *antidiabetic activity of TT-ZnONPs*

In this study, 30 healthy Sprague-Dawley mice (28±2g, 5-6 weeks old), comprising both males and females, were procured for induction of diabetes with alloxan monohydrate solution at 180 mg/kg, body weight from the University of Veterinary and Animal Sciences, Lahore. Mice received a 10% glucose mixture immediately after alloxan to avoid immediate low blood sugar. Blood sugar levels were monitored before and after the alloxan administration. Mice with glucose levels higher than 150 mg/dl were identified as diabetic and chosen for the study (Vanitha and Karthikeyan 2013). These mice were divided into six groups, each containing 5 as follows: Group A: untreated negative control; Group B: untreated diabetic control; Group C: treated with glibenclamide (standard drug as positive control) at 10mg/Kg; Group D: treated with TT-ZnONPs at 10mg/Kg; Group E: treated with TT-ZnONPs at 20mg/Kg; Group F: treated with TT-ZnONPs at 30mg/Kg.

Mean body weight (MBW) and blood glucose level were evaluated on days 1, 7, 14, 21, and 28. Subsequently, mice were anesthetized with a ketamine-xylazine mixture (80mg/kg and 150 mg/kg, respectively) following an overnight fast (Bayrami *et al*., 2020). Samples of blood were collected in tubes with EDTA for the assessment of biochemical and hematological parameters. The liver, kidney, and pancreas were surgically excised, preserved in 10% formalin, and further processed using the paraffin wax infiltration method.

Biochemical analysis of blood

The serum isolated from the blood samples was processed further for the estimation of components of lipid profile *viz.* triglyceride (STG), cholesterol (STC), low-density lipoprotein cholesterol (LDL-C), very low-density lipoprotein cholesterol (VLDL-C), and high-density lipoprotein cholesterol (HDL-C), liver function test *viz.* alanine aminotransferase (ALT), aspartate aminotransferase (AST), alkaline phosphatase (ALP), bilirubin, and total protein), and renal function test (urea, uric acid, creatinine, and albumin) using the Beckman Coulter AU680 analyzer (Jarhahzadeh *et al*., 2021).

Analysis of hematological parameters

Hematological assessment was conducted on blood samples collected in EDTA-containing tubes using a Beckman Coulter LH 750 hematology analyzer, following the manufacturer's guidelines. The parameters evaluated include red blood cell count (RBCs), white blood cell count (WBCs), hemoglobin (Hb), mean corpuscular hemoglobin (MCH), mean corpuscular hemoglobin concentration (MCHC), haematocrit (HCT), and mean corpuscular volume (MCV) (Rieger *et al*., 2021).

Histopathological analysis

The fixed tissues were prepared for wax embedding and cutting section at 6µm, which were later stained with hematoxylin and eosin. Then, the histological preparations were analyzed for diabetic and treatment effects (Silva-Santana *et al*., 2020).

Statistical analysis

The data were analyzed to determine the Mean±SEM and group differences assessed using the Two-Way ANOVA Bonferroni test through GraphPad Prism 5.0 software. Statistical significance was attributed to a p-value < 0.05.

RESULTS

Characterization of TT-ZnONP

Figure 1 shows the characterization of TT-ZnONPs prepared and used in this study. The shift in mixture color from green-yellow to pale white throughout the reaction provided evidence for the preparation of nanoparticles. Moreover, phytochemicals may also be involved in a reduction mechanism of Zn^{2+} to Zn^{O} ions.

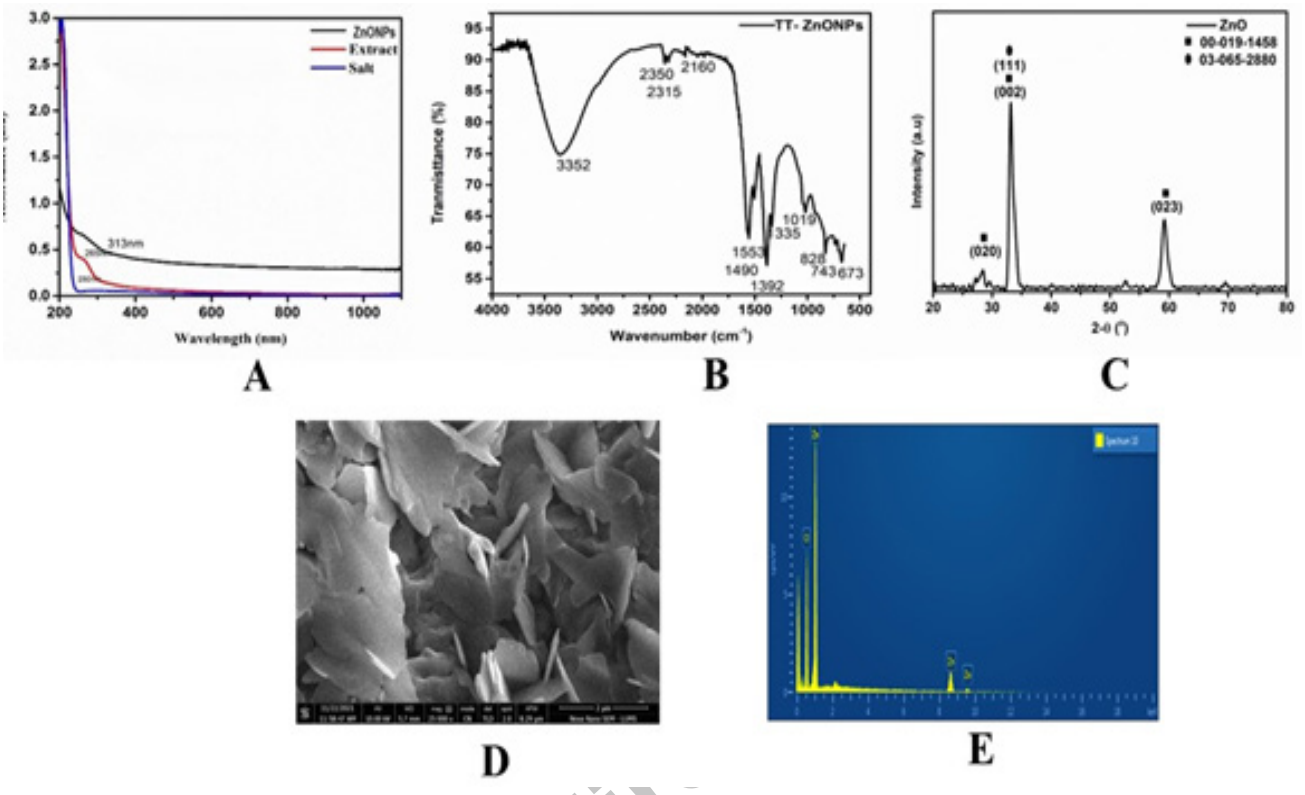

Fig. 1. Characterization of TT-ZnONPs. (A) UV-Vis absorption peak observed at 313 nm that is also consistent with published research indicating an absorption peak of ZnO at 320 nm, (B) According to FTIR data, interactions between the hydroxyl group, carboxylic group, carbonyl group, amines, and the flavonoids present in the TTFE extract may have stabilized the produced ZnONPs, (C) Pure monoclinic and cubic phase of ZnO structure (JCPDS 03-065-2880) were Identified by the XRD pattern as having braggs reflection peaks at 28.5°, 33.5°, 33.5° and 58.9° which attributed to the crystal plane of (0 2 0), (0 0 2), (111) and (0 2 3), respectively (D) By using SEM analysis, it can be observed that unveil haphazardly stacked thin nanosheets having petal like morphology, (E) EDX profile displays a robust signal indicating the existence of zinc and oxygen atoms participating in the surface encapsulation of NPs.

The UV-Vis absorption of salt, extract, and NPs was observed. TTFE exhibited an SPR peak value at 265 nm which correlates well with the results of Gopinath *et al*. (2016) where it was confirmed at 280 nm SPR. Furthermore, the absorption band was observed at 313 nm in the case of TT-ZnONPs, whereas earlier findings show an absorption peak of ZnO at 320 nm (Liu *et al*., 2019).

The effect of bioactive compounds in *T. terrestris* extract on the synthesis of ZnONPs was studied with the help of FTIR spectroscopy. Bands emerged at around 3352 cm^{-1}, 2350 cm^{-1}, 2315 cm^{-1}, 2160 cm^{-1}, 1490 cm^{-1}, 1392 cm^{-1}, 1335 cm^{-1}, 1019 cm^{-1}, 828 cm^{-1}, 743 cm^{-1} and 673 cm^{-1}. The peak at 3380cm^{-1} represented the stretching of hydroxyl groups in the amide and the bending of C-N in amide was represented by a peak at 1560 cm^{-1}. The presence of peaks around 2350 cm^{-1} showed amino group stretching while the peak at 2315 cm^{-1} indicated the stretching mode of CH of hydrocarbon. The peak at 2160 cm^{-1} was also characteristic of alkenes stretching while the peak at 1490 cm^{-1} was related to the elongation of C–C bonds within the benzene ring. The peak at around 1335 cm^{-1} and 1393 cm^{-1} was associated with the bending and movement of the primary and secondary alcohol functional groups. Furthermore, the bands at 1019 cm^{-1}, 828 cm^{-1}, and 743 cm^{-1} could be correlated to the deformations of the amine C-N groups. The minor band at 664 cm^{-1} may associated with a chlorinated alkyl group and the cubic phase of ZnONPs.

The XRD pattern of TT-ZnONPs showed 2θ peaks at 28.5°, 33.5°, 33.5°, and 58.9° which were attributed to the crystal planes of (0 2 0), (0 0 2), (111), and (0 2 3), respectively. All the diffraction peaks corresponded to the precursor of zinc (hydrozincite) (JCPDS 00-019-1458) and the pure monoclinic and cubic phases of ZnO structure (JCPDS 03-065-2880) (Bitenc and Orel, 2009; Jose *et al*., 2020; Sabzi *et al*., 2018). The crystal size of ZnONPs was 4.67 nm.

Table I. Effect of *Tribulus terrestris*-synthesized zinc oxide nanoparticles (TT-ZnONPs) on the body weight of normal and diabetic mice.

Groups	A	B	C	D	E	F
Day 0	29.8±0.3	28.4±0.8	28.6±0.9	29.2±0.9	30.8±0.6	29.8±1.0
Day 7	29.0±0.8	26.4±1.2	28.4±0.6	29.0±1.0	30.4±0.6$^{\#\#}$	30±0.3$^{\#}$
Day 14	30.2±0.8	23.8±0.8***	30±1.0$^{\#\#\#}$	29.2±0.9$^{\#\#\#}$	31.6±1.0$^{\#\#\#}$	30±0.4$^{\#\#\#}$
Day 21	29.8±1.0	19.6±1.5***	29.2±0.8$^{\#\#\#}$	29.8±0.5$^{\#\#\#}$	31.2±0.8$^{\#\#\#}$	30.6±1.0$^{\#\#\#}$
Day 28	30.6±0.9	15.2±0.5***	30.6±0.5$^{\#\#\#}$	30.4±0.5$^{\#\#\#}$	31±0.3$^{\#\#\#}$	31.4±0.9$^{\#\#\#}$

Two-way ANOVA followed by Bonferroni test. Data expressed as Mean±SEM (n=5). *p<0.05, **p<0.01, ***p<0.001 vs Group A; $^{\#}$p<0.05, $^{\#\#}$p<0.01, $^{\#\#\#}$p<0.001 vs Group B. Group A, untreated negative control; Group B, untreated diabetic control; Group C, treated with glibenclamide at 10mg/kg; Group D: treated with TT-ZnONPs at 10 mg/kg; Group E, treated with TT-ZnONPs at 20 mg/kg; Group F, treated with TT-ZnONPs at 30 mg/kg.

Table II. Effect of TT-ZnONPs on the blood glucose levels of normal and diabetic mice.

Groups	A	B	C	D	E	F
Day 0	103.8±5.4	315.0±18.1***	327.2±23.6	314.8±22.9	319.4±33.3	331.0±32.5
Day 7	107.0±1.7	321.2±21.8***	306.0±19.6	287.0±21.0	291.6±33.4	295.0±31.7
Day 14	98.4±3.8	354.2±22.8***	296.4±19.6	253.0±21.0$^{\#\#}$	239.0±14.5$^{\#\#\#}$	227.0±17.1$^{\#\#\#}$
Day 21	120.2±3.0	362.2±23.7***	279.2±12.4$^{\#}$	222.0±18.2$^{\#\#\#}$	208.0±18.8$^{\#\#\#}$	165.0±13.0$^{\#\#\#}$
Day 28	105.4±2.2	392.4±32.7***	267.0±12.9$^{\#\#\#}$	205.0±18.0$^{\#\#\#}$	154.0±10.1$^{\#\#\#}$	148.6±9.9$^{\#\#\#}$

See Table I for statistical details and details of groups.

The SEM image revealed haphazardly stacked thin nano-sheets with a petal-like morphology. The length of the sheet was approximately 1.5 µm. An EDX assessment was performed to determine their constituent elements. It confirmed the existence of zinc and oxygen signals within TT-ZnONPs and this analysis revealed peaks related to the optical absorbance of the resulting NPs. The elemental composition assessment of the NPs revealed 80% zinc and 19% oxygen composition, confirming the high purity of the produced NP. These results aligned with previous studies (Raj and Jayalakshmy, 2015).

Evaluation of TT-ZnONPs anti-diabetic activity

After 28 days of treatment, diabetic mice showed decreased MBW (15.2 ± 0.5) compared to control (30.6 ± 0.9 g) but the treatment with glibenclamide and 10, 20 and 30 mg/kg TT-ZnONPs significantly increased the level of MBW to 30.6 ± 0.5, 30.4 ± 0.5, 31 ± 0.3 and 31.4 ± 0.9 g, respectively (Table I).

Similarly, at the end of treatment, blood glucose levels (BGLs) significantly increased in diabetic mice (392.4 ± 32.7) compared to control (105.4 ± 2.2) but the treatment with glibenclamide and 10, 20 and 30 mg/kg TT-ZnONPs significantly and dose-dependently decreased the BGLs to 267.0 ± 12.9, 205.0 ± 18.0, 154.0 ± 10.1 and 148.6 ± 9.9, respectively (Table II).

Effect of TT-ZnONPs on lipid profile

The values of biochemical parameters including lipid profile, liver function test (LFT), and renal function test (RFT) in all the groups were recorded. Contrary to the normal control group (74.4±3.9), diabetic mice showed significantly higher serum levels of STC (205±8.8). Treatment with glibenclamide (10 mg/kg) and 10, 20 and 30 mg/kg of TT-ZnONPs significantly and dose-dependently decreased the level of STC to 177±5.3, 149±14.0, 125±9.4 and 119±5.7, respectively (Table III).

Similarly, in control, serum STG (85.4±4.2) was significantly lower than the diabetic mice (199±17.9). Treatment with glibenclamide and 10, 20 and 30 mg/kg TT-ZnONPs significantly and dose-dependently decreased the level of STG to 166±13.1, 153.6±10.0, 135±6.8, and 132±6.2, respectively.

In normal control (41.0±5.7), diabetic mice showed significantly higher serum levels of LDL-c (141.2±2.5). Treatment with glibenclamide and 10, 20 and 30 mg/kg TT-ZnONPs significantly decreased the level of LDL-c from141.2±2.5 to 115±4.0, 106.8±5.8, 111±6.3 and 104±6.7, respectively.

Compared with the normal control (17.6±0.8), diabetic mice showed significantly higher serum levels of VLDL-c (63.2±3.7). Treatment with glibenclamide and 10, 20 and 30 mg/kg TT-ZnONPs significantly and dose-dependently decreased the level of VLDL-c to 27±1.9, 29.9±2.5, 29.8±2.2 and 27±1.7, respectively.

Table III. Effect of TT-ZnONPs on the lipid profile, liver function, and renal function parameters in normal and diabetic mice.

Groups	A	B	C	D	E	F
Lipid profile (mg/dl)						
STC	74.4±3.9	205±8.8***	177±5.3$^{\#\#}$	149±14.0$^{\#\#\#}$	125±9.4$^{\#\#\#}$	119±5.7$^{\#\#\#}$
STG	85.4±4.2	199±17.9***	166±13.1$^{\#}$	153.6±10.0$^{\#\#\#}$	135±6.8$^{\#\#\#}$	132±6.2$^{\#\#\#}$
LDL-c	41.0±5.7	141.2±2.5***	115±4.0$^{\#}$	106.8±5.8$^{\#\#}$	111±6.3$^{\#}$	104±6.7$^{\#\#}$
VLDL-c	17.6±0.8	63.2±3.7***	27±1.9$^{\#\#}$	29.9±2.5$^{\#}$	29.8±2.2$^{\#\#}$	27±1.7$^{\#\#}$
HDL-c	57.2±3.6	14.8±1.2***	40±4.2$^{\#}$	47.2±3.6$^{\#\#}$	49.6±2.6$^{\#\#}$	54±3.2$^{\#\#\#}$
LFTs						
ALT (IU/l)	62.6±3.41	169±9.8***	123±8.0$^{\#\#}$	108.0±7.6$^{\#\#\#}$	92.0±6.5$^{\#\#\#}$	82±3.08$^{\#\#\#}$
AST (IU/l)	53.4±4.7	319.6±10.7***	286.4±6.0$^{\#}$	176.2±12.9$^{\#\#\#}$	108±3.7$^{\#\#\#}$	87.8±2.9$^{\#\#\#}$
ALP (IU/l)	163.4±14.1	406.0±2.3***	361±14.8$^{\#\#}$	258.0±15.9$^{\#\#\#}$	233±5.5$^{\#\#\#}$	210±7.3$^{\#\#\#}$
Bilirubin (mg/dl)	0.76±0.05	3.06±0.1***	1.2±0.1$^{\#\#\#}$	1.28±0.08$^{\#\#\#}$	1.0±0.1$^{\#\#\#}$	1.0±0.05$^{\#\#\#}$
T. protein (g/dl)	6.90±0.34	2.64±0.3***	5.1±0.5$^{\#\#\#}$	5.52±0.2$^{\#\#\#}$	6.6±0.2$^{\#\#\#}$	6.3±0.2$^{\#\#\#}$
RFTs (mg/dl)						
Urea	29.0±3.5	54.6±3.9***	47±2.8	37.8±2.3$^{\#\#\#}$	34.0±2.6$^{\#\#\#}$	29±0.8$^{\#\#\#}$
Uric acid	18.8±1.3	32.4±1.9***	25.4±1.8	23.2±1.3$^{\#}$	19.0±1.7$^{\#\#\#}$	21.8±0.8$^{\#\#}$
Creatinine	0.7±0.1	2.1±0.2***	1.0±0.2$^{\#\#}$	0.9±0.1$^{\#\#\#}$	0.7±0.1$^{\#\#\#}$	0.8±0.0$^{\#\#\#}$
Albumin	4.0±0.4	2.1±0.1***	3.1±0.1$^{\#\#}$	3.5±0.1$^{\#\#\#}$	3.8±0.3$^{\#\#\#}$	4.0±0.2$^{\#\#\#}$

See Table I for statistical details and details of groups. STC, serum total cholesterol (mg/dl); STG, serum triglycerides (mg/dl); LDL-c, low-density lipoprotein cholesterol (mg/dl); VLDL-c, very low-density lipoprotein cholesterol (mg/dl); HDL-c, high-density lipoprotein cholesterol; LFTs, liver function tests; ALT, alanine aminotransferase; AST, aspartate aminotransferase; ALP, alkaline phosphatase; T protein, total protein and RFTs, renal function tests.

The normal control group showed significantly higher serum levels of HDL-c (57.2±3.6) as compared to diabetic (14.8±1.2). Treatment with glibenclamide and 10, 20 and 30 mg/kg TT-ZnONPs significantly and dose-dependently increased the level of HDL-c to 40±4.2, 47.2±3.6, 49.6±2.6 and 54±3.2, respectively.

Effect of TT-ZnONPs on liver function biomarkers

To evaluate the effect of TT-ZnONPs on liver function, liver function biomarkers (ALT, AST, ALP, bilirubin, and total proteins) were measured in an untreated diabetic group and treatment groups. The data demonstrated that the level of ALT, AST, ALP, and bilirubin was considerably elevated in untreated diabetic mice in contrast to the normal control group (Table III). Administration of 10mg/kg glibenclamide (standard drug) significantly decreased the levels of aforesaid liver function biomarkers. Next, we measured the level of these biomarkers in the TT-ZnONPs treated group. The data showed that TT-ZnONPs significantly decreased the level of these biomarkers in a dose-dependent fashion (Table III). It is important to mention that the suppressive effect of TT-ZnONPs on serum levels of ALT, AST, ALP, and bilirubin was more profound as compared to glibenclamide.

On the other hand, total protein declined to a significant level in diabetic mice (2.64±0.3) as compared to control (6.90±0.34). Administration of 10mg/kg glibenclamide significantly increased total protein (5.1±0.5). In the group treated with 10, 20 and 30 mg/kg TT-ZnONPs, total protein level increased to 5.52±0.2, 6.6±0.2, and 6.3±0.2, respectively.

Effect of TT-ZnONPs on renal function biomarkers

To evaluate the impact of TT-ZnONPs treatment on renal function, we measured the levels of urea, uric acid, creatinine, and albumin. As shown in Table III, the level of urea, uric acid, and creatinine increased significantly in untreated diabetic mice compared to normal control. Administration of 10 mg/kg glibenclamide significantly decreased the level of urea, uric acid, and creatinine. Similarly, the TT-ZnONPs treatment significantly decreased the level of urea, uric acid, and creatinine in diabetic mice in a dose-dependent way.

On the other hand, a decrease in albumin levels was observed in untreated diabetic mice compared to control. Administration of 10mg/kg glibenclamide significantly increased albumin. In the group treated with 10, 20 and 30 mg/kg TT-ZnONPs, albumin increased dose-dependently as shown in Table III.

Table IV. Effect of TT-ZnONPs on hematological parameters in normal and diabetic mice.

Groups	A	B	C	D	E	F
RBCs (10^6µl)	8.5±0.4	1.5±0.1***	4.4±0.5	7.5±0.3$^{\#\#}$	7.7±0.2$^{\#\#}$	8.7±0.2$^{\#\#\#}$
WBCs (10^3µl)	8.0±0.5	2.8±0.3*	6.9±0.1	8.1±0.2$^{\#}$	8.0±0.2$^{\#}$	10.2±0.3$^{\#\#\#}$
Hb (g/dl)	15.1±0.4	7.5±0.9***	12.5±0.4$^{\#}$	13.5±0.5$^{\#\#}$	15.4±0.3$^{\#\#\#}$	16.5±0.2$^{\#\#\#}$
MCH (pg)	24.9±0.9	12.2±0.7***	17.8±1.1$^{\#}$	22.4±1.0$^{\#\#\#}$	26±0.8$^{\#\#\#}$	27.8±0.8$^{\#\#\#}$
MCHC (g/dl)	33.8±0.7	22.8±1.1***	29.4±0.6$^{\#\#}$	32.4±0.9$^{\#\#\#}$	34.6±0.7$^{\#\#\#}$	35.8±0.8$^{\#\#\#}$
HCT (%)	44.2±2.8	25.0±1.7***	25.2±1.9	41.6±3.0$^{\#\#\#}$	44.4±1.4$^{\#\#\#}$	47.8±1.3$^{\#\#\#}$
MCV (fl)	53.6±1.9	29.0±1.4***	35.2±2.2$^{\#\#}$	41.6±1.1$^{\#\#\#}$	56.4±2.0$^{\#\#\#}$	63.8±2.9$^{\#\#\#}$

See Table I for statistical details and details of groups. RBCs, red blood cells; WBCs, white blood cells; Hb, hemoglobin; MCH, mean corpuscular hemoglobin; MCHC, mean corpuscular hemoglobin concentration; HCT, hematocrit and MCV, mean corpuscular volume.

Effect of TT-ZnONPs on hematological parameter

Diabetic mice show a significant decrease in the levels of RBCs WBCs, Hb, MCH, MCHC, HCT, and MCV. However, treatment with 10, 20 and 30mg/kg TT-ZnONPs improved the number of RBCs, WBCs, Hb, MCH, MCHC, HCT, and MCV as indicated in Table IV.

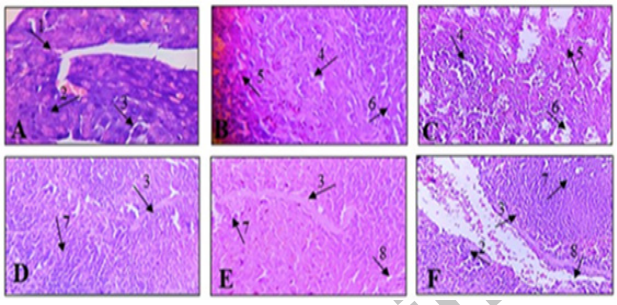

Fig. 2. Effect of different doses of TT-ZnONPs treatment on histological structure of pancreas of altoxan induced diabetic mice. 1: normal IL; 2: normal intralobular duct; 3: normal blood vessels; 4: shrinkage of IL; 5: infiltration of lymphocytes; 6: hypochromatosis and the disappearance of cell borders in the IL; 7 decreased infiltrations of lymphocytes; 8: repaired IL. (A) untreated negative control, (B) untreated diabetic group, (C) treated with glibenclamide at 10mg/kg, (D) treated with TT-ZnONPs at 10mg/kg, (E) treated with TT-ZnONPs at 20mg/kg, and (F) treated with TT-ZnONPs at 30mg/kg. Stain: H & E; Magnification: 40X.

Effect of TT-ZnONPs on histopathology of pancreas, liver and kidney

Based on the microscopic examination of the pancreas, it was noted that the control group has a fully developed pancreas, normal Islets of Langerhans (IL) with proper cell membrane. The histological abnormalities in the glibenclamide-treated group were comparable to those in the diabetic group, which shows extensive damage to the islet cells, and few number of islet cells. However, in the 10, 20 and 30 mg/kg TT-ZnONPs treated group, the number and shape of islet islets were nearly standard with some cell degeneration in the middle which indicates that the hypoglycemia effect of ZnONPs was connected to healed pancreatic tissue injury (Fig. 2).

Liver histology revealed that the normal control group showed typical lobular morphology with central vein (CV), normal hepatocytes, sinusoids, and hepatic artery in control. In contrast, diabetic untreated mice showed shrinkage of the CV, distorted hepatocytes, severe congestion, and dilatation in sinusoids and portal veins. Treatments with glibenclamide and 10mg/kg ZnONPs restored the appearance of hepatocytes, CV, and slight sinusoidal dilation. However, treatment with 20 and 30 mg/kg TT-ZnONP showed marked improvements in the distorted hepatocytes, CV, and sinusoids (Fig. 3).

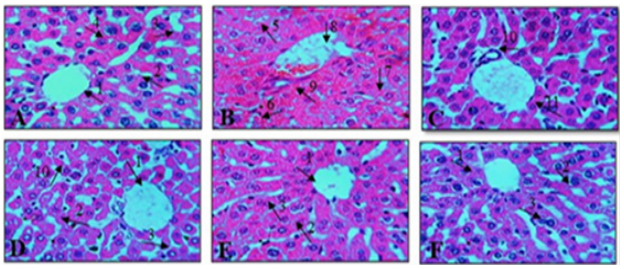

Fig. 3. Effect of different doses of TT-ZnONPs treatment on histological structure of liver of altoxan induced diabetic mice. 1: normal CV; 2: normal hepatocytes arrangements; 3: sinusoids; 4: hepatic artery; 5: shrinkage of the CV; 6: degeneration of hepatocytes; 7: hepatic sinusoidal congestion and dilation; 8: Intense portal vein dilatation and congestion; 9: inflammation-related cell infiltrations within the fibrous tract; 10: mild degeneration of hepatocyte; 11: mild congested CV. For details of treatments in A, B, C, D, E, F see Fig. 2. Stain: H & E; Magnification: 40X.

Kidney histology revealed normal renal corpuscle

components in normal control. In contrast, diabetic untreated mice showed distorted and shrunken glomerulus, necrosis, vacuolization, and enlargement of the renal tubule epithelial cell. Treatment with glibenclamide showed minimum improvement in renal corpuscles (glomerulus and Bowman's capsule), necrosis, and expansion of the renal tubule epithelial cells. Treatment with 10 and 20 mg/kg ZnONPs showed moderate improvement in renal corpuscles (glomerulus and Bowman's capsule), mild necrosis, and mild expansion in renal tubule epithelial cells. Treatment with 30 mg/kg ZnONPs showed marked improvement in in renal corpuscles (glomerulus and Bowman's capsule), mild necrosis and tubule epithelial cells did not exhibit any signs of swelling (Fig. 4).

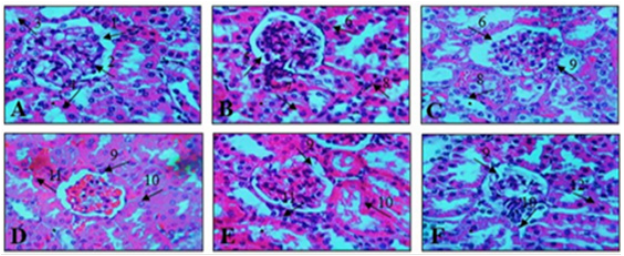

Fig. 4. Effect of different doses of TT-ZnONPs treatment on histological structure of kidney of altoxan induced diabetic mice. 1: bowman's capsule; 2: normal glomeruli; 3: proximal convoluted ducts; 4: distal convoluted ducts; 5: degeneration of glomeruli; 6: necrosis; 7: vacuolarization of renal cells; 8: swelling in the renal tubule epithelial cells; 9: improvement of glomeruli; 10: mild necrosis; 11: mild swelling is seen in the renal tubule epithelial cells; 12: normal renal tubule epithelial cells. For details of treatments in A, B, C, D, E, F, see Fig. 2. Stain: H & E; Magnification: 40X.

DISCUSSION

Our findings suggest a significant hypoglycemic effect of synthesized TT-ZnONPs. Various mechanisms could explain the hypoglycemic action of ZnONPs. *T. terrestris* contains alkaloids, flavonoids, polyphenols, glycosides, tannins, and significant saponins, which demonstrate an inhibitory effect against α-glucosidase and enhance insulin-dependent diabetes symptoms. The herb exhibited hypoglycemic characteristics and possesses a substantial hydroalcoholic content, contributing to the reduction of serum glucose, STG, and STC levels. Moreover, it has been shown to enhance coronary blood flow in individuals with DM. This study reported, for the first time that TT-ZnONPs have a hypoglycemic effect in the body. Color changes during synthesis, UV-VIS spectra peaks, FTIR functional group analysis, XRD crystal structure confirmation, SEM morphology observations, and EDX elemental composition analysis all validated the production of high-purity TT-ZnONPs. These results suggested the promising biomedical and pharmaceutical applications for TT-ZnONP.

One of the main characteristics of DM is weight loss, which is often associated with the breakdown of structural proteins and muscle atrophy. This study demonstrated that inducing diabetes with alloxan is correlated with a significant reduction in MBW. The most prevalent symptoms of DM were elevated BGLs or hyperglycemia resulting from the pancreas's inability to produce insulin or from insulin resistance. This study revealed that BGLs significantly increased after alloxan administration in mice. However, upon the administration of TT-ZnONPs, a substantial, dose-dependent decrease in BGLs was observed. Comparable outcomes regarding BGLs have also been documented previously (Ahmed *et al*., 2022).

Contrasting with the normal control, diabetic mice showed significantly higher serum levels of STG, STC, VLDL-c, LDL-c, and lower HDL-c levels in lipid profile which are frequently associated with hyperlipidemia. Lack of insulin during the diabetic condition causes the body's many regulatory and metabolic systems to become out of whack. In a healthy condition, insulin triggers the lipolytic hormones to break down triglycerides in the peripheral fat depots and stop the release of free fatty acids. Lipoprotein lipase aids in the liver's transformation of free fatty acids into phospholipids and cholesterol compounds before being discharged into the blood. However, it is inactivated by insulin insufficiency, leading to a high serum phospholipid level. Treatment with TT-ZnONPs significantly decreased the levels of STG, STC, VLDL-c, and LDL-c while increasing HDL-c levels. This suggested that TTFE might possess insulin-like effects, which reduce the frequency of problems caused by lipids. Similar effects were also reported for lipid profile with leaves of *Passiflora incarnate* in mice with diabetes induced by STZ (Gupta *et al*., 2012).

In people with persistent DM, liver injury is also fairly common. By disrupting the metabolism of lipids, carbohydrates, and proteins, persistent DM can induce non-alcoholic fatty liver disease. Subsequently, this condition can progress to non-alcoholic steatohepatitis, liver fibrosis, and eventually, the development of hepatocellular carcinomas by stimulating an inflammatory reaction to oxidative stress. Patients with DM demonstrate increased levels or activities of hepatic enzymes as a result of liver damage. Treatment with TT-ZnONPs caused a significant decrease in ALT, AST, ALP, and bilirubin levels and elevated total protein. A remarkable increase in the liver function enzymes with leaf infusion from *Wedelia*

chinensis in mice with alloxan-induced diabetes was also reported (Bari *et al*., 2020).

A renal system problem, such as diabetic nephropathy, is also brought on by DM. The results of this investigation demonstrated that, in contrast to albumin, diabetic mice demonstrated increased serum levels of urea, uric acid, and creatinine, three key markers of renal dysfunction. Treatment with TT-ZnONPs significantly decreased urea, uric acid, and creatinine whereas significantly increased albumin levels. In a previous study, *Berberis calliobotrys* was found to substantially reduce urea and creatinine levels in diabetic rats (Rasool *et al*., 2023).

Hematological measurements also revealed information about the level of hemolysis and bone marrow activity. The current study demonstrated that the group of diabetics who were not receiving treatment for their condition had abnormal hematological characteristics. This might be caused by the destruction of matured RBCs, which results in low hemoglobin count (Hb) (because of the reaction of excess glucose with the Hb to give rise to glycosylated hemoglobin), decrease in RBCs (an indication of its synthesis and destruction being out of balance), and HCT typically being affected by alloxan-induced diabetic mice, an indication of anemia. Additionally, while the MCH, MCHC, and MCV levels are related to individual RBC, the WBC levels in the untreated diabetic group may be a sign that the immune system's ability to fend off foreign invaders is waning. Treatment with TT-ZnONPs caused a significant increase in the level of RBCs, WBCs, Hb, MCH, MCHC, HCT, and MCV as indicated in Table IV. 10 mg/kg glibenclamide showed no significant effect for RBCs, WBCs and HCT counts while significant effect on Hb, MCH, MCHC and MCV counts. The more significant effect showed by the administration of 30 mg/kg TT-ZnONPs on all these hematological parameters. Ajiboye and Ojo (2014) also reported similar effects for these hematological parameters with aqueous leaf infusion of *Senecio biafrae* in mice with alloxan-induced diabetes.

The histological examination of pancreatic, liver, and kidney tissues revealed significant improvements with TT-ZnONP treatment across all doses, indicating potential therapeutic benefits for diabetes-related tissue damage. Pancreatic tissues showed recovery of islet morphology and reduced cell degeneration, while liver and kidney tissues exhibited improvements in hepatocyte and renal corpuscle morphology, respectively. These findings suggested a promising role for TT-ZnONPs in ameliorating tissue damage associated with diabetes. Previous research has also shown the protective effects of plant-mediated nanoparticles on the pancreas, liver and kidney (Kazmi *et al*., 2021; Rahman *et al*., 2023).

CONCLUSION

The current research findings suggested that various doses of TT-ZnONPs exhibit antidiabetic activity. TT-ZnONPs demonstrated the potential to improve MBW, BGLs, and transition from hyperlipidemia to normolipidemia in a dose-dependent manner due to their antidiabetic properties. Furthermore, biochemical and histological analyses indicated the pancreatic, hepatic, nephrotic, and hematic protective effects of TT-ZnONPs in alloxan-induced diabetic mice. These results provided valuable insights for the development of future food supplements aimed at mitigating the effects of diabetes-related issues.

DECLARATION

Funding

No funding was acquired for this project.

Ethical approval

The *in vivo* experiments were performed with ethical approval from the Ethics Committee of the Zoology Department, Government College University, Lahore, Pakistan with reference no. GCU/IIB/938. All animal trials followed both local and global methods following the guidelines established in accordance with regulations set forth by the Animal Research regulating authority, institutional guidelines, and Article 9 of the Wet op de dierproeven (Dutch law, internationally). The animals were managed following the guidelines specified in the "Guide for the Care and Use of Laboratory Animals" from the National Institute of Health (NIH) Publication (NRC 2011).

Statement of conflict of interest

The authors have declared no conflict of interest.

REFERENCES

Ahmed, S.S., Alqahtani, A.M., Alqahtani, T., Alamri, A.H., Menaa, F., Mani, R.K., DR, B. and Kavitha, K., 2022. Green synthesis, characterizations of zinc oxide nanoparticles from aqueous leaf extract of Tridax procumbens Linn. and Assessment of their anti-hyperglycemic activity in streptozoticin-induced diabetic rats. *Materials*, **15**: 8202. https://doi.org/10.3390/ma15228202

Ajiboye, B.O. and Ojo, O.A., 2014. Effect of aqueous leaf extract of Senecio biafrae on hyperglycaemic and haematological parameters of alloxan-induced diabetic rats. *Pharmacol. Online,* **3**: 163–169.

Amin, A.M.R., Lotfy, M., Shafiullah, M. and Adeghate, E., 2006. The protective effect of *Tribulus terrestris* in diabetes. *Ann. N. Y. Acad. Sci.,* **1084**: 391–401. https://doi.org/10.1196/annals.1372.005

Azeem, A.M. and Abd-el-Megid, M.H., 2023. Assessment of the biogenic effects of selenium nanoparticles prepared from citrus paradise peel extract against bisphenol a-induced liver injury in male rats. *Pakistan J. Zool.*, **55**: 2317-2323. https://doi.org/10.17582/journal.pjz/20210901220942

Bari, M.W., Islam, M.M., Khatun, M., Sultana, M.J., Ahmed, R., Islam, A., Hossain, M.I., Rahman, M.M. and Islam, M.A., 2020. Antidiabetic effect of Wedelia chinensis leaf extract in alloxan induced Swiss albino diabetic mice. *Clin. Phytosci.,* **6**: 1–8. https://doi.org/10.1186/s40816-020-00197-6

Bayrami, A., Haghgooie, S., Pouran, S.R., Arvanag, F.M. and Habibi-Yangjeh, A., 2020. Synergistic antidiabetic activity of ZnO nanoparticles encompassed by Urtica dioica extract. *Adv. Powder Technol.,* **31**: 2110–2118. https://doi.org/10.1016/j.apt.2020.03.004

Bitenc, M. and Orel, Z.C., 2009. Synthesis and characterization of crystalline hexagonal bipods of zinc oxide. *Mater. Res. Bull.,* **44**: 381–387. https://doi.org/10.1016/j.materresbull.2008.05.005

Bonakdaran, A., Fallah Huseini, H., Khalighi-Sigaroodi, F., Abdoli, M. and Ahvazi, M., 2008. Investigation of the hypoglycemic effect of *Tribulus terrestris* extract on diabetic rats. *J. Med. Pl.,* **7**: 85–92.

Bouzekri, A., Slimani, S., Nassar, M., Zaaboub, S. and Sakhraoui, N., 2024. Potential mitigation of spirotetramat-induced reproductive toxicity by *Tribulus terrestris* in domestic pigeons (*Columba livia* domestica). *Pakistan J. Zool.*, **56**: 1403-1413. https://doi.org/10.17582/journal.pjz/20220420130439

Chandrakala, V., Aruna, V. and Angajala, G., 2022. Review on metal nanoparticles as nanocarriers: Current challenges and perspectives in drug delivery systems. *Emergent Mater.,* **5**: 1593–1615. https://doi.org/10.1007/s42247-021-00335-x

DiSanto, R.M., Subramanian, V. and Gu, Z., 2015. Recent advances in nanotechnology for diabetes treatment. *Wiley Interdiscip. Rev. Nanomed. Nanobiotechnol.,* **7**: 548–564. https://doi.org/10.1002/wnan.1329

Gopinath, V., Priyadarshini, S., Al-Maleki, A.R., Alagiri, M., Yahya, R., Saravanan, S. and Vadivelu, J., 2016. *In vitro* toxicity, apoptosis and antimicrobial effects of phyto-mediated copper oxide nanoparticles. *RSC Adv.,* **6**: 110986–110995. https://doi.org/10.1039/C6RA13871C

Gupta, R.K., Kumar, D., Chaudhary, A.K., Maithani, M. and Singh, R., 2012. Antidiabetic activity of *Passiflora incarnata* Linn. in streptozotocin-induced diabetes in mice. *J. Ethnopharmacol.,* **139**: 801–806. https://doi.org/10.1016/j.jep.2011.12.021

Hameed, S., Khalil, A.T., Ali, M., Iqbal, J., Rahman, L., Numan, M., Khamlich, S., Maaza, M., Ullah, I. and Abbasi, B.A., 2021. Precursor effects on the physical, biological, and catalytic properties of *Fagonia indica* Burm. f. mediated zinc oxide nanoparticles. *Microsc. Res. Tech.,* **84**: 3087–3103. https://doi.org/10.1002/jemt.23867

Jarhahzadeh, M., Alavinejad, P., Farsi, F., Husain, D. and Rezazadeh, A., 2021. The effect of turmeric on lipid profile, malondialdehyde, liver echogenicity and enzymes among patients with nonalcoholic fatty liver disease: A randomized double blind clinical trial. *Diabetol. Metab. Syndr.,* **13**: 1–9. https://doi.org/10.1186/s13098-021-00731-7

Jose, L.M., Kuriakose, S. and Thomas, S., 2020. Fabrication, characterization and *in vitro* antifungal property evaluation of biocompatible lignin-stabilized zinc oxide nanoparticles against selected pathogenic fungal strains. *Bionanoscience,* **10**: 583–596. https://doi.org/10.1007/s12668-020-00748-8

Kamtekar, S. and Keer, V., 2014. Management of diabetes: A review. *Res. J. Pharm. Technol.,* **7**: 1065–1072.

Kazmi, S.A.R., Qureshi, M.Z., Sadia, Alhewairini, S.S., Ali, S., Khurshid, S. and Mughal, T.A., 2021. Minocycline-derived silver nanoparticles for assessment of their antidiabetic potential against alloxan-induced diabetic mice. *Pharmaceutics*, **13**: 1678. https://doi.org/10.3390/pharmaceutics13101678

Khan, H. S., Tariq, M., Mukhtar, T. and Gulzar, A., 2021. Insecticidal toxicity of plant extracts and green silver nanoparticles against Aedes albopictus. *Pakistan J. Zool.*, **53**: 2123-2128. https://doi.org/10.17582/journal.pjz/20191214051208

Liu, Z., Chen, F. and Lu, Z., 2019. Biofabrication of zinc oxide nanoparticles, characterization and cytotoxicity against pediatric leukemia cell lines. *Green Process. Synth.*, **9**: 56–62. https://doi.org/10.1515/gps-2020-0007

Rahman, A., Rehman, G., Shah, N., Hamayun, M., Ali, S., Ali, A. and Alrefaei, A.F., 2023. Biosynthesis and characterization of silver nanoparticles using *Tribulus terrestris* seeds: Revealed promising antidiabetic potentials. *Molecules*, **28**: 4203. https://doi.org/10.3390/molecules28104203

Raj, L.F.A. and Jayalakshmy, E., 2015. Biosynthesis and characterization of zinc oxide nanoparticles using root extract of *Zingiber officinale*. *Orient. J. Chem.,* **31**: 51–56. https://doi.org/10.13005/ojc/310105

Rajam, R.P., 2024. A review on trends in nano technology–new era in diabetes treatment. *Int. J. Green Pharm.*, **18**: 39-49.

Rasool, S., Al-Meslmani, B. and Alajlani, M., 2023. Determination of hypoglycemic, hypolipidemic and nephroprotective effects of berberis calliobotrys in alloxan-induced diabetic rats. *Molecules*, **28**: 3533. https://doi.org/10.3390/molecules28083533

Rieger, J., Pelckmann, L.M. and Drewes, B., 2021. Preservation and processing of intestinal tissue for the assessment of histopathology. In: *Animal models of allergic disease: Methods and protocols.* pp. 267–280. https://doi.org/10.1007/978-1-0716-1001-5_18

Sabzi, M., Far, S.M. and Dezfuli, S.M., 2018. Characterization of bioactivity behavior and corrosion responses of hydroxyapatite-ZnO nanostructured coating deposited on NiTi shape memory alloy. *Ceram. Int.,* **44**: 21395–21405. https://doi.org/10.1016/j.ceramint.2018.08.197

Shafey, A.M., 2020. Green synthesis of metal and metal oxide nanoparticles from plant leaf extracts and their applications: A review. *Green Proc. Synth.*, **9**: 304–339. https://doi.org/10.1515/gps-2020-0031

Silva-Santana, G., Bax, J.C., Fernandes, D.C.S., Bacellar, D.T.L., Hooper, C., Dias, A.A.S.O., Silva, C.B., de Souza, A.M., Ramos, S. and Santos, R.A., 2020. Clinical hematological and biochemical parameters in Swiss, BALB/c, C57BL/6 and B6D2F1 Mus musculus. *Anim. Model Exp. Med.,* **3**: 304–315. https://doi.org/10.1002/ame2.12139

Simos, Y.V., Spyrou, K., Patila, M., Karouta, N., Stamatis, H., Gournis, D., Dounousi, E. and Peschos, D., 2021. Trends of nanotechnology in type 2 diabetes mellitus treatment. *Asian J. Pharm. Sci.,* **16**: 62–76. https://doi.org/10.1016/j.ajps.2020.05.001

Stefanescu, R., Farczadi, L., Huțanu, A., Ősz, B.E., Mărușteri, M., Negroiu, A. and Vari, C.E., 2021. Tribulus terrestris efficacy and safety concerns in diabetes and erectile dysfunction, assessed in an experimental model. *Plants*, **10**: 744. https://doi.org/10.3390/plants10040744

Vanitha, M. and Karthikeyan, J., 2013. Evaluation of aloevera gel for its anti-inflammatory activity in diabetes mellitus using animal model system. *Int. J. Drug Dev. Res.,* **5**: 305–309.

Virk, P., 2018. Anti-diabetic activity of green gold-silver nanocomposite with trigonella foenum graecum L. seeds extract on streptozotocin-induced diabetic rats. *Pakistan J. Zool.*, **50**: 711-718. https://doi.org/10.17582/journal.pjz/2018.2.711.718